Physicomechanical, Optical, Barrier, and WAXS Studies of Filled Linear Low-Density Polyethylene Films

Siddaramaiah,[1] T. Jeevananda,[1] K. S. Jagadeesh,[2] H. Somashekarappa,[3] R. Somashekar[3]

[1]*Department of Polymer Science and Technology, Sri Jayachamarajendra College of Engineering, Mysore 570 006, India*
[2]*JSS Academy of Technical Education, Noida 201301 (UP), India*
[3]*Department of Studies in Physics, University of Mysore, Mysore 570 006, India*

Received 27 September 2002; accepted 24 February 2003

ABSTRACT: Linear low-density polyethylene (LLDPE) with different fillers such as silica, mica, and soy protein isolate were compounded using a single screw extruder and blown into films by a Konark blow-film machine. The filled LLDPE films were characterized for physicomechanical and optical properties. Barrier properties such as water vapor transmission rate and oxygen transmission rate of the filled LLDPE films were also reported. Microcrystalline parameters such as crystal size ($\langle N \rangle$) and lattice distortion (g in %) of the filled LLDPE films were estimated from the wide-angle X-ray scattering method using Hosemann's paracrystalline model. © 2003 Wiley Periodicals, Inc. J Appl Polym Sci 90: 2938–2944, 2003

Key words: WAXS; structure–property relations; films; barrier; fillers

INTRODUCTION

Plastic packaging has aroused enormous interest in the field of packing technology for a wide spectrum of advantages they offer over traditional packing materials like wood, paper, and metal, for instance. Thermoplastic materials, especially because of their superior properties, have been posing a strong challenge to conventional packing materials.[1–3] Among thermoplastic materials, polyolefins are extensively used in packing industries because of easy availability, processability, flexibility, and excellent optical and seal strength. In addition, no other ingredients are required during processing of polyolefins. This has paved the way for investigations on these thermoplastic materials in terms of physicomechanical, barrier, and other properties by incorporating various fillers, blending, and copolymerization.[4–8] Several investigators have studied the effect of different fillers like mica, silica, calcium carbonate, titanium oxide, and alumina on performance of these materials.[4–11] The effect of $KMnO_4$ on properties of low-density polyethylene (LDPE) films for packaging of fresh fruits and vegetables was reported by Ramakrishna et al.[12]

To select the polymer material for suitable packing application, in-depth knowledge of structure–property relationships of modified polymers is required from materials technologists. However, the effect of fillers on barrier properties and wide angle X-ray scattering (WAXS) studies of linear low-density polyethylene (LLDPE) films have not been the focus of much research. In this investigation fillers like mica, silica, and soy protein isolate (SPI) were incorporated into LLDPE using a twin-screw extruder. Some of the physicomechanical and optical properties of filled LDPE and LLDPE films were published in our earlier study.[11] In continuation of our previous work this study deals with the structure–property relations of filled LLDPE films.

EXPERIMENTAL

Materials

LLDPE (specifications: density, 0.92 g/cm^3; melt flow index, 2 g/10 min; melting point, 115–125°C) used in this investigation was obtained from M/s. IPCL, Baroda, India. The fillers used were mica [practical (P)], mica [commercial (C)], silica, and SPIs, obtained from M/s. Ranbaxy Laboratories, New Delhi, India, and were used without further purification. All the fillers had an average particle size of about 15 μm.

Compounding and film blowing of filled LLDPE

LLDPE was compounded with the fillers using a Haake twin-screw extruder (CTW 100; Bersdorff, Germany) with L/D ratio 33 : 1. A temperature profile of 156–180°C was maintained during the process. The compounded LLDPE was then blown into 75-μm-thick films using a Konark single-screw extruder with

Correspondence to: Siddaramaiah (siddaramaiah@yahoo.com).

Journal of Applied Polymer Science, Vol. 90, 2938–2944 (2003)

L/D ratio 22 : 1. Film blowing was done at a temperature profile of 170–190°C.

Techniques

Mechanical properties like tensile strength and percentage elongation at break were measured using an Instron universal testing machine (Model 4302; Instron, Canton, MA) according to ASTM D-882. Elemendorf tear strength was determined according to ASTM D-1922. A minimum of five samples were tested at room temperature for each composition and the average values reported. Optical properties like percentage transmission of light and haze were measured according to ASTM D-1003 using a Suga test hazemeter (Model 206). The water vapor transmission rate (WVTR) and oxygen transmission rate (OTR) were measured according to ASTM D-96 and ASTM D-1434-66, respectively.

X-ray recording and profile analysis

X-ray diffraction data on films were collected on a Stoe/Stadi-P powder diffractometer (Bragg–Brento geometry) with germanium monochromated radiation of Cu–K_α ($\lambda = 1.5406$ Å) in a transmission mode, using a curved position-sensitive detector in the 2θ ranges from 5 to 30° at a scan rate of 4°/min. The intensity was corrected for Lorentz polarization factors and also for instrumental broadening using the Stokes deconvolution method.[13]

We estimated parameters such as crystal size ($\langle N \rangle$) and increase in strain (lattice disorder, g in %) by simulating the X-ray profile by employing the procedure described in previous studies[14–17] for Bragg reflections at $2\theta \approx 21.3$ and 23.6°.

The simulation of intensity profile was carried out on the basis of Hosemann's one-dimensional linear paracrystalline model and the equations used for this purpose are given below.[18] The scattered intensity is

$$I\,(\mathrm{s}) = I_{N-1}\,(\mathrm{s}) + I_N^1\,(\mathrm{s}) \tag{1}$$

where

$$I_N\,(\mathrm{s}) = 2\mathrm{Re}\langle (1 - I^{N+1})/(1 - I) + [I\nu/d(1 - I)^2]\{I^N[N(1 - I) + 1] - 1\}\rangle^{-1} \tag{2}$$

where $\nu = 2ia^2s + d$, $I = I_1\,(\mathrm{s}) = \exp(-a^2s^2 + ids)$, and $a^2 = \omega^2/2$.

$I_N^1\,(\mathrm{s})$, the modified intensity for the probability peak centered at D, is given by

$$I_N^1\,(\mathrm{s}) = \frac{2a_N}{D(\pi)^{1/2}} \exp(iDs) \times \{1 - a_N s[2D(a_N s) + I(\pi)^{1/2}\exp(-a_N^2 s^2)]\} \tag{3}$$

where $a_N^2 = N\omega^2/2$, ω is the standard deviation of the nearest-neighbor probability function,[17,19] and $D(a_N s)$ is the Dawson's integral or the error function with purely complex argument and can be computed. $\langle N \rangle$ is the number of unit cells counted in a direction perpendicular to the (hkl) Bragg plane, g is the lattice strain given by $\Delta d/d$ ($=\omega/d$), d is the spacing of the (hkl) planes, Re refers to the real part of the expression, and a is related to the standard deviation ω is the lattice distribution function. The experimental profile between s_0 and $s_0 + s_0/2$ (or s_0 and $s_0 +$ B2d, if there is truncation of the profile $B < 1$ and $B = 1$, when there is no truncation, $d = d_{\mathrm{hkl}}$) is matched with corresponding simulated order of reflection between the calculated and experimental normalized intensity values. SIMPLEX is a multidimensional algorithm[19] used for minimization. This method gives reliable values of $\langle N \rangle$ and g and was also used recently for estimating the microstructural parameters for materials in a round-robin test conducted by IUCr, UK.

Using this procedure, values of the crystal size ($\langle N \rangle$) and lattice strain (g) were obtained for X-ray reflections at 2θ of 21.3 and 23.6°. Here d_{hkl} is the perpendicular distance from the origin to the hkl plane and ω is the standard deviation of the probability distribution associated with the distortion of the lattice [related to the strain by $g^2 = (\omega/d)^2$]. Here, $s = (\sin\theta)/\lambda$ and s_0 is the scattering vector corresponding to the peak of the X-ray profile. Here, the surface-weighted (D_{sur}) crystal size is given by the integral [20]

$$D_{\mathrm{surf}} = \frac{\int_0^\pi LP_s(L)\,dL}{\int_0^\pi P_s(L)\,dL} \tag{4}$$

and

$$P_s(L)\alpha[\delta^2 A_s(n)/\delta L^2] \tag{5}$$

RESULTS AND DISCUSSION

Physicomechanical properties

The physicomechanical properties of all the filled LLDPE films are given in Table I. Some of these data were previously published elsewhere.[11] It is clearly evident from the table that with the incorporation of fillers, the tensile strength of the film decreased in accordance with reported observations.[2,9,21] The percentage elongation at break value decreases from 157% for unfilled LLDPE film to 112% for 3% mica (commercial)–filled LLDPE film.

Tear strength is a significant property for high-capacity pouches, bags, and other industrial applica-

TABLE I
Physicomechanical and Optical Properties of Pure LLDPE and Filled LLDPE Systems

Sample	Tensile strength ± 2% (kg/cm^2)	Percentage Elongation at break ± 2% (%)	Tear strength ± 2% (g)	Burst strength ± 1% (kg/cm^2)	Percentage Transmittance ± 2% (%)	Haze ± 2%
LLDPE	270	157	108	0.62	49.7	38.7
LLDPE + 0.75% silica	218	142	156	0.93	38.0	44.0
LLDPE + 2% mica (P)	166	129	362	0.60	37.2	25.1
LLDPE + 2% mica (C)	151	123	215	0.42	28.5	66.2
LLDPE + 3% mica (P)	159	118	319	0.58	42.2	48.9
LLDPE + 3% mica (C)	135	112	202	0.38	30.2	58.8
LLDPE + 1% SPI	138	144	92	0.52	31.0	45.7

tions. LLDPE has an average tear strength of 108 *g* and it increases with the addition of filler except for 1% soy protein isolate. This is attributed to the fact that the fillers act as obstructions for tear propagation.[22]

Optical properties

Optical properties—percentage transmittance and haze values—of the filled LLDPE films are given in Table I. LLDPE had an average percentage transmittance of 49.7% and haze value of 38.7. As expected, percentage transmittance of the LLDPE films decreased with the incorporation of fillers from 49.7 to 28.5%. It may also be observed that haze values increased with the addition of fillers from 38.7 to 66.2, which is attributed to the scattering of light by particulate fillers.[23–26]

Barrier properties

In food-packaging industries, permeability to water vapor and gases (particularly oxygen) critically decides the protective property of the plastic films. Varied permeability values are also desired in certain applications like modified-atmosphere packing. LLDPE had an average WVTR of 7.60 g/m^2 and OTR of 6450 cm^3/m^2. The changes in WVTR and OTR values after incorporation of different fillers are presented in Table II. It may be observed from Table II that WVTR declined in filled films compared to unfilled LLDPE film, which may be attributed to the weakening of intermolecular forces in the polymer with the incorporation of fillers. However, the value remains the same as that of pure LLDPE for the 3% mica (P) system. From this we may say that a water-sensitive product can be stored in a 3% mica–filled system to achieve high self-life of the product. The OTR value for filled films increased from 6450 to 7450 cm^3/m^2.

X-ray profile analysis

Representative X-ray diffractograms of pure and filled LLDPE systems are given in Figure 1 (a)–(d). It is evident from Figure 1(a) that LLDPE film shows two prominent sharp reflections at (2θ) 21.41° (110) and 23.7° (200), whereas that of the SPI-filled system shows peaks at (2θ) 21.47° (110) and 23.63° (200), respectively. It may also be observed from the diffractograms that a gradual broadening and shifting of the peaks occurred after incorporating fillers. This is attributed to the rearrangement of the net plane structure, which is controlled by the value of g, the lattice strain.[22,27]

For the sake of completeness we have reproduced in Figure 2(a)–(d) the simulated and experimental profiles for both pure and filled systems. In fact the goodness of fit was less than 2% in all the samples, thus showing that the model used here is quite reliable.

Various microcrystalline parameters like number of crystal size ($\langle N \rangle$), smallest crystallite size (p), width of the crystal size distribution (α), lattice strain (g in %), enthalpy (α^*), interplanar distance (d_{hkl}), and surface-weighted crystal size (D_S) were calculated using the equations reported in the literature[11] and are tabulated in Table III.

From Table III it may be seen that there are significant changes in the crystal size ($\langle N \rangle$) values after the filler loading, attributed to reorganization of the polymer network. To put the results in a better perspective, we projected these results to a common x– y plane, using the relation

TABLE II
Barrier Properties of Pure LLDPE and Filled LLDPE Systems

Sample	WVTR ± 2%[a] (g/m^2)	OTR ± 2%[b] (cm^3/m^2)
LLDPE	7.60	6450
LLDPE + 0.75% silica	6.20	7120
LLDPE + 2% mica (P)	6.90	7180
LLDPE + 2% mica (C)	7.20	7160
LLDPE + 3% mica (P)	7.60	7250
LLDPE + 3% mica (C)	6.85	7450
LLDPE + 1% SPI	5.90	7050

[a] Conditions: 24 h at 38°C and 90% RH.
[b] Conditions: 24 h at 27°C and 65% RH.

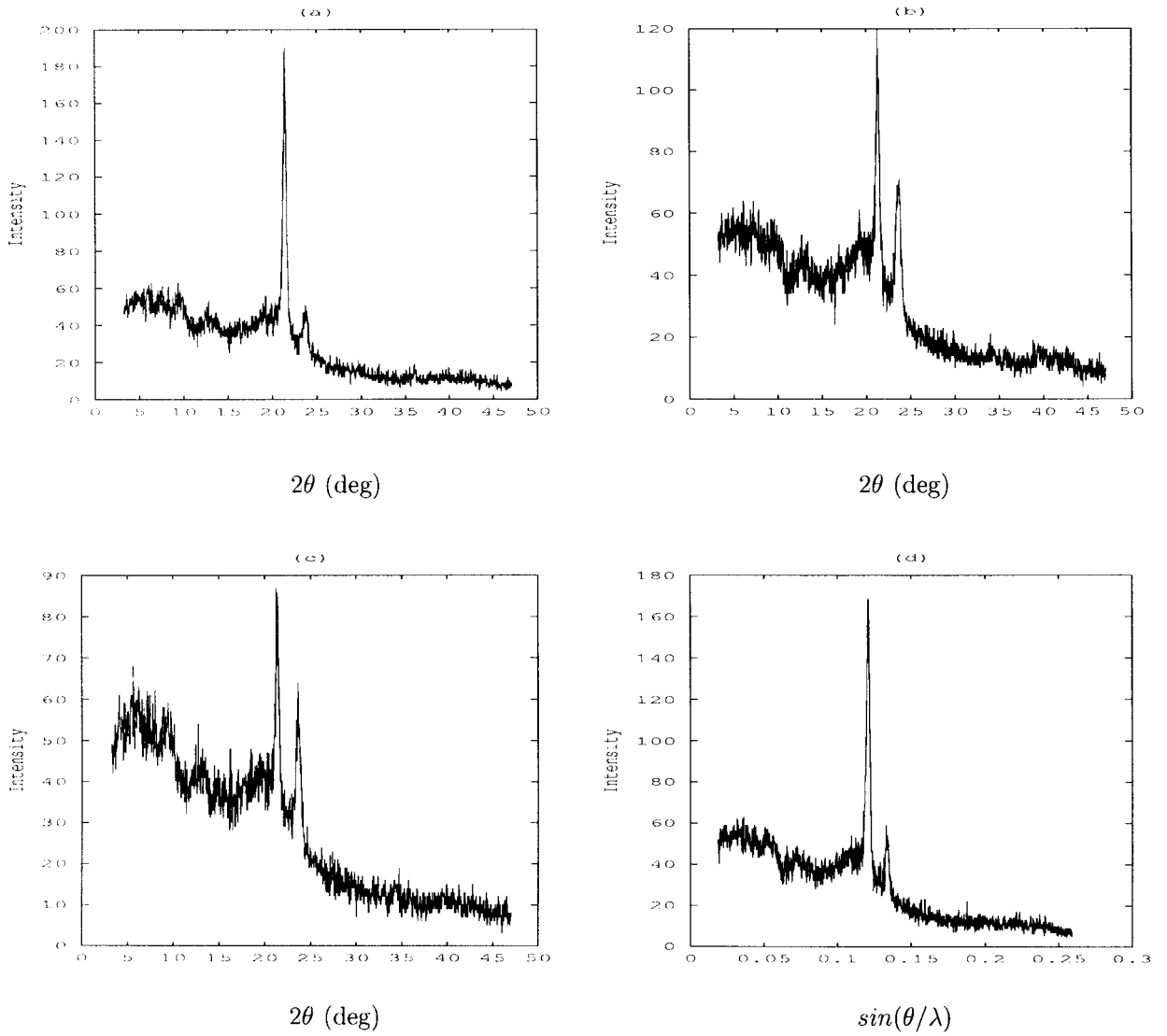

Figure 1 Wide-angle X-ray diffractograms of (a) LLDPE, (b) LLDPE + 2% mica (P), (c) LLDPE + 2% mica (C), and (d) LLDPE + 1% SPI.

$$\left(\frac{2}{N_{\text{hkl}}}\right)^2 = \left(\frac{\cos(\theta)}{y}\right)^2 + \left(\frac{\sin(\theta)}{x}\right)^2 \tag{6}$$

and fitted the crystal size values of LLDPE into an ellipsoid shape with D along the x-axis and y_{min} was obtained from an iteration procedure using the crystal size data of all other relations observed in that particular sample. Here θ is the angle between the two (hkl) planes and D is the crystal size corresponding to the particular (hkl) reflection. Figure 3 shows a comparison of ellipsoid shapes [(1)–(5)] of crystallites of pure and filled LLDPE samples. According to Hosemann's model, these changes in crystal size values and ellipsoid shapes are attributed to the interplay between the strain present in the polymer network and the number of unit cells coherently contributing to the X-ray reflection.

From the parameters like crystal size and lattice strain, we can estimate the minimum enthalpy (α^*), which defines the equilibrium state of microparacrystals in filled LLDPE films using the relation[27]

$$\alpha^* = \langle N \rangle^{1/2} g \tag{7}$$

This α^* value implies physically that the growth of paracrystals in a particular material is appreciably controlled by the level of g in the net plane structure. The estimated values of enthalpy are also given in Table III. The average value of α^* for LLDPE is 0.23; moreover, the nature of the filler incorporated into LLDPE does not alter the value of α^* (within experimental error), implying the phase stabilization of the filled system. This conclusion was drawn on the basis of the minimum value of α^* (0.23), the enthalpy that is

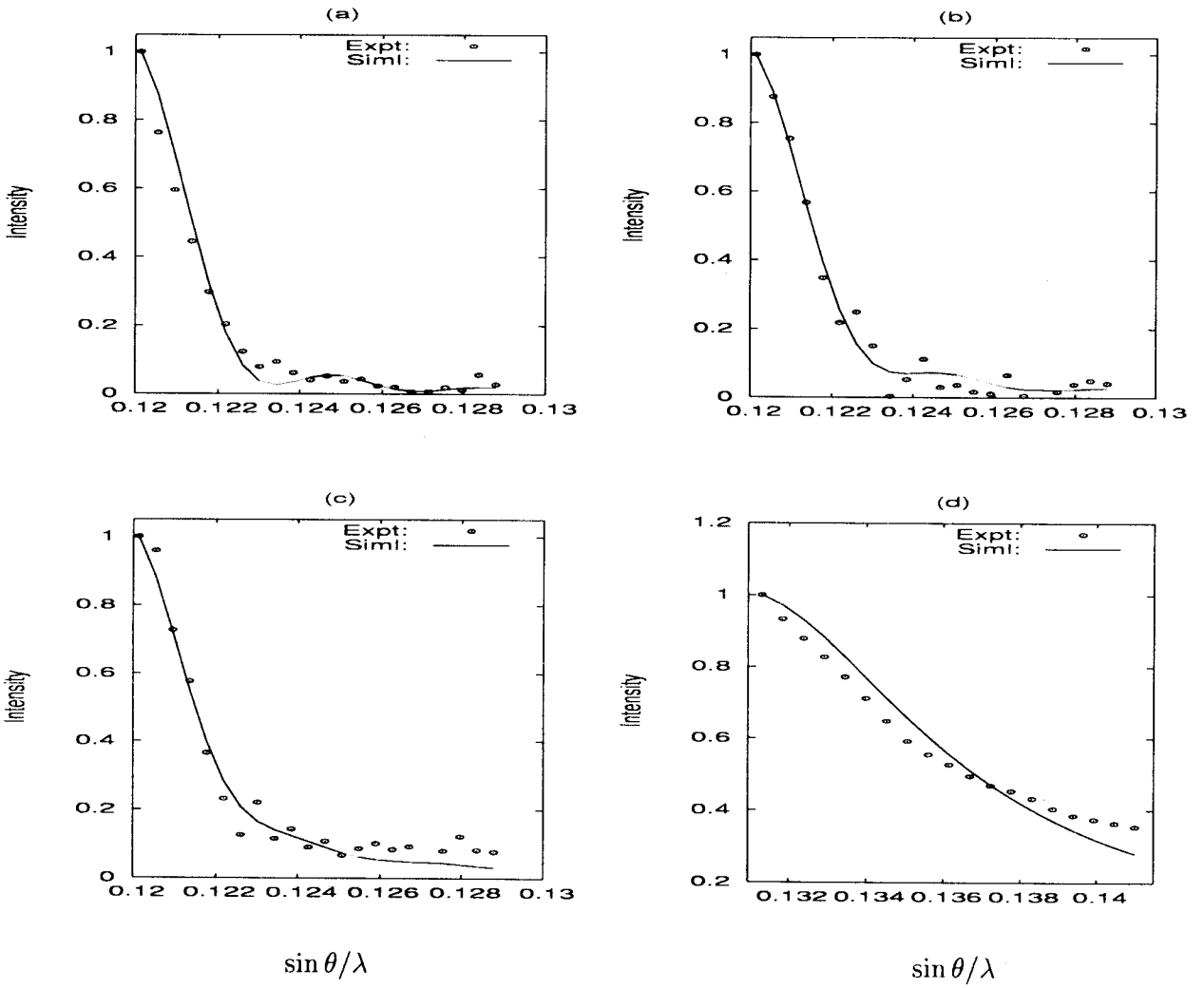

Figure 2 Experimental and simulated profiles for (a) LLDPE, (b) LLDPE + 2% mica (P), (c) LLDPE + 2% mica (C), and (d) LLDPE + 1% SPI.

a measure of the energy required for the formation of the net plane structure, and is in agreement with the values reported by Hosemann[27] for polymers.

From Table III it may be observed that there is a marginal increase in lattice strain (g in %) value after incorporation of filler to LLDPE. The reason for such a

TABLE III
Microcrystalline Parameters of Pure LLDPE and Filled LLDPE Systems

Sample	2θ (°)	$\langle N \rangle$	p	α	g (in %)	α^*	d_{hkl} (Å)	D_s (Å)
LLDPE	21.41	46.36 ± 0.91	46.35	—	3.35 ± 0.1	0.23	4.15	192.40
	23.70	30.16 ± 0.5	23.47	0.150	4.86 ± 0.1	0.27	3.75	146.58
LLDPE + 0.75% silica	21.33	25.77 ± 0.2	13.90	0.084	4.74 ± 0.7	0.24	4.16	107.20
	23.60	27.77 ± 0.5	19.05	0.113	4.31 ± 0.1	0.23	3.77	105.15
LLDPE + 2% mica (P)	21.29	19.64 ± 0.2	10.68	0.112	5.40 ± 0.1	0.24	4.17	81.90
	23.75	28.84 ± 0.3	28.75	—	5.01 ± 0.1	0.27	3.74	107.86
LLDPE + 2% mica (C)	21.33	26.75 ± 0.3	26.71	—	5.12 ± 0.1	0.26	4.16	111.18
	23.63	30.17 ± 0.5	23.45	0.149	4.05 ± 0.1	0.22	3.75	113.14
LLDPE + 3% mica (P)	21.41	27.13 ± 0.2	14.67	0.080	4.14 ± 0.1	0.22	4.15	112.59
	23.72	32.23 ± 0.5	32.21	—	4.92 ± 0.1	0.28	3.75	120.86
LLDPE + 3% mica (C)	21.32	24.42 ± 0.3	24.42	0.060	5.42 ± 0.1	0.27	4.49	101.59
	23.63	23.52 ± 0.1	11.72	0.085	3.79 ± 0.1	0.18	3.75	88.24
LLDPE + 1% SPI	21.47	43.88 ± 0.7	43.87	0.090	4.57 ± 0.1	0.30	4.14	181.47
	23.63	22.13 ± 0.2	14.84	0.137	6.49 ± 0.1	0.31	3.75	83.00

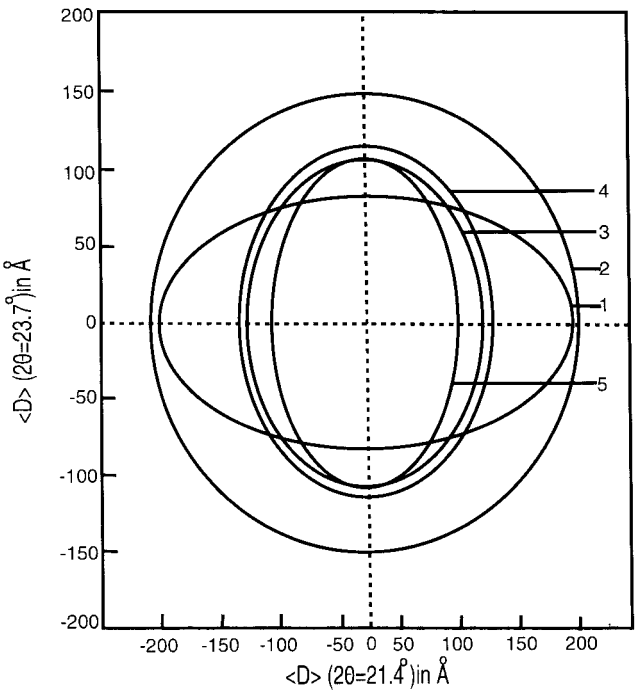

Figure 3 Ellipsoid shape of crystallites of (1) LLDPE + 1% SPI, (2) LLDPE, (3) LLDPE + 0.75% silica, (4) LLDPE + 2% mica (C), and (5) LLDPE + 2% mica (P).

change can be attributed to indiscriminate filler granules in the matrix of LLDPE, which generally tends to lower the short-range interaction between the layers of LLDPE leading to an increase in disorder of the lattice. These changes result in increased broadening of X-ray reflections. It may also be observed from the table that the reduction in crystal size ($\langle N \rangle$), smallest crystal unit (p), and surface-weighted crystal size (D_S) values after incorporation of filler to LLDPE. This can be attributed to the organizational changes in the polymer network.

Table III also indicates that there are no significant changes in α^* and d_{hkl} values for both Bragg reflections after incorporation of fillers. Width of the crystallite distribution function (α) changes with the incorporation of fillers, indicating reorganization of the polymer network. Even though we have quantified the changes in the LLDPE-filled system using X-ray profile analysis, we were able to obtain only an average picture of the relation between the mechanical properties with the structure.

On a macroscopic scale mechanical properties such as tensile strength and percentage elongation at break show a marginal reduction where crystal size, the smallest crystal unit, and D_S values are very low. Variations of these properties with crystal size are given in Figure 4(a)–(c), where the straight line is a consequence of statistical analysis carried out to ascertain the nature of changes in physical parameters with crystal size; it may be observed that there is a very weak correlation between these two variables in this context.

CONCLUSIONS

The following conclusions can be drawn from this study:

- Incorporation of different fillers into LLDPE resulted in a decrease of tensile strength and percentage elongation at break, which may be attributed to the reduction in intramolecular interaction between the polymer networks.
- Slight decreases in water vapor transmission rate and a marginal increase in oxygen transmission rate were observed after incorporation of fillers into the LLDPE system.

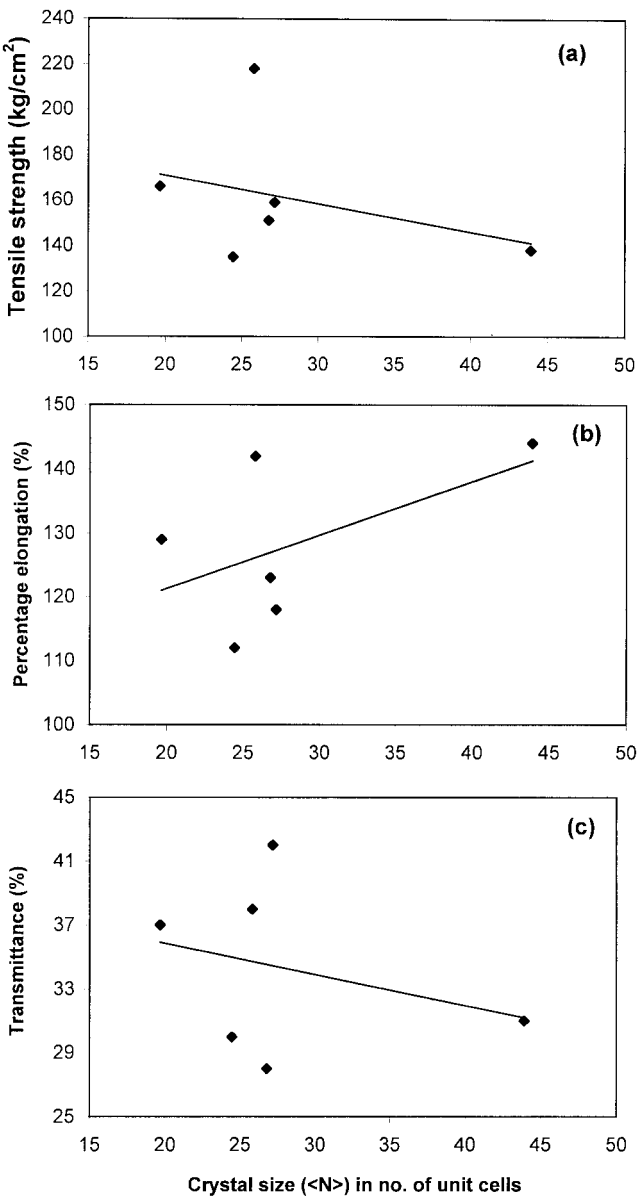

Figure 4 Variation of (a) tensile strength, (b) % elongation at break, and (c) % transmittance with crystal size for filled LLDPE systems.

- X-ray profile analysis of filled LLDPE reveals that the changes in the physical properties are essentially attributable to rearrangement of the polymer network, with a new set of microstructural parameters computed using broadened profiles.
- Different fillers, which alter the shape of the crystallite and hence the polymer networks, lead to changes in physical properties.

References

1. Figg, K. Packaging Technol Sci 1989, 2, 215.
2. Gennadoise, A.; Weller, C. L.; Tesin, R. F. Cereal Chem 1993, 70, 426.
3. Kemper, E. L.; Bahl, K. S. J Plast Film Sheet 1994, 10, 336.
4. Robert, B. S. U.S. Pat. 4,336,301, 1982.
5. Vick, C. S.; Fairhurst, D. Plast Compos 1984, 7, 2.
6. Seymour, R. B.; Carraher, C. E. Structure Property Relation in Polymers; Plenum Press: New York, 1984.
7. Gordienko, V. P. Kempoz Polim Mater 1985, 27, 58.
8. Skripachav, V. I.; Kuznetsov, V. I.; Ivanchev, S. S. Plast Mater 1985, 3, 16.
9. Radosta, J. A. J Plast Film Sheet 1991, 7, 181.
10. Schumpt, H. P.; Bilogan, W. Kunststoffe 1993, 73, 6.
11. Siddaramaiah; Nagarahalli, R. T.; Ramakrishna, A.; Varadarajulu, A. J Plast Film Sheet 1997, 13, 252.
12. Ramakrishna, A.; Kumar, R.; Srivatsa, A. N. In: Proceedings of IFCON'98, 4th International Food Convention, India, 1998.
13. Stokes, A. R. Proc Phys Soc London 1948, 61, 382.
14. Press, W.; Flannery, B. P.; Teukolsky, S.; Vettering, W. T. Numerical Recipes; Cambridge University Press: Cambridge, UK, 1988; p. 284.
15. Somashekar, R.; Hall, I. H.; Carr, P. D. J Appl Cryst 1989, 22, 363.
16. Hall, I. H.; Somashekar, R. J Appl Cryst 1991, 24, 1051.
17. Silver, M. M.S. Thesis, UMIST, UK, 1988.
18. Wilson, A. J. C. Elements of X-ray Crystallography; Addison–Wesley: Reading MA, 1970; p. 191.
19. Press, W.; Flannery, B. P.; Teukolskey, S.; Vetterling, W. T., Eds. Numerical Recipes; Cambridge University Press: Cambridge, UK, 1986; pp. 83–85.
20. Balzar, D. J Res Natl Stand Technol 1993, 88, 32.
21. Chacko, V. P.; Farris, R. J.; Karasz, F. E. J Appl Polym Sci 1983, 28, 2701.
22. Puffr, R.; Sebendra, J. J Polym Sci C 1967, 16, 79.
23. Wang, G. C.; Wang, J. X.; Zhangs, Z. P. Polym Int 1991, 25, 237.
24. Siddaramaiah; Mallu, P.; Somashekhar, R. J Appl Polym Sci 1998, 68, 1739.
25. Khanna, Y. P.; Day, E. D.; Tsai, M. L.; Vaidyanathan, G. J Plast Film Sheet 1997, 13, 197.
26. Demorest, R. L. J Plast Film Sheet 1997, 13, 197.
27. Hosemann, R. Colloid Polym Sci 1982, 268, 982.